TOUGH-FLAC: A NUMERICAL SIMULATOR FOR ANALYSIS OF COUPLED THERMAL-HYDROLOGIC-MECHANICAL PROCESSES IN FRACTURED AND POROUS GEOLOGICAL MEDIA UNDER MULTI-PHASE FLOW CONDITIONS

Jonny Rutqvist and Chin-Fu Tsang

Lawrence Berkeley National Laboratory
Earth Sciences Division
Berkeley, CA 945 30, USA
e-mail: JRutqvist@lbl.gov

ABSTRACT

This paper presents development of a simulator for coupled thermal-hydrological-mechanical (THM) processes in fractured porous geological media and recent applications of the simulator related to coupled THM processes under multiphase flow conditions. The simulator is denoted TOUGH-FLAC because it utilizes two established computer codes—TOUGH2 and FLAC3D—which are linked and jointly executed for analysis of coupled thermal-hydrologic-mechanical (THM) processes. Capabilities of the TOUGH-FLAC simulator are demonstrated on several complex coupled problems related to injection and storage of carbon dioxide in aquifers and to disposal of nuclear waste in unsaturated fractured porous media.

THE TOUGH-FLAC THM SIMULATOR

The TOUGH-FLAC simulator (Rutqvist et al. 2002) is based on a coupling of the two existing computer codes TOUGH2 (Pruess et al. 1999) and FLAC3D (Itasca Consulting Group 1997). TOUGH2 is a well-established code for geohydrological analysis with multiphase, multicomponent fluid flow and heat transport, while FLAC3D is a widely used commercial code that is designed for rock and soil mechanics. For analysis of coupled THM problems, the TOUGH2 and FLAC3D are executed on compatible numerical grids and linked through external coupling modules, which serve to pass relevant information between the field equations that are solved in respective code (Figure 1 and 2).

TOUGH-FLAC COUPLING MODULES

A TOUGH to FLAC link takes multiphase pressures, saturation, and temperature from the TOUGH2 simulation and provides updated temperature, and pore pressure to FLAC3D (Figure 1). Because a TOUGH2 mesh uses one gridpoint within each element, and FLAC3D nodes are located in element corners, data have to be interpolated from mid-element (TOUGH2) to corner locations (FLAC3D).

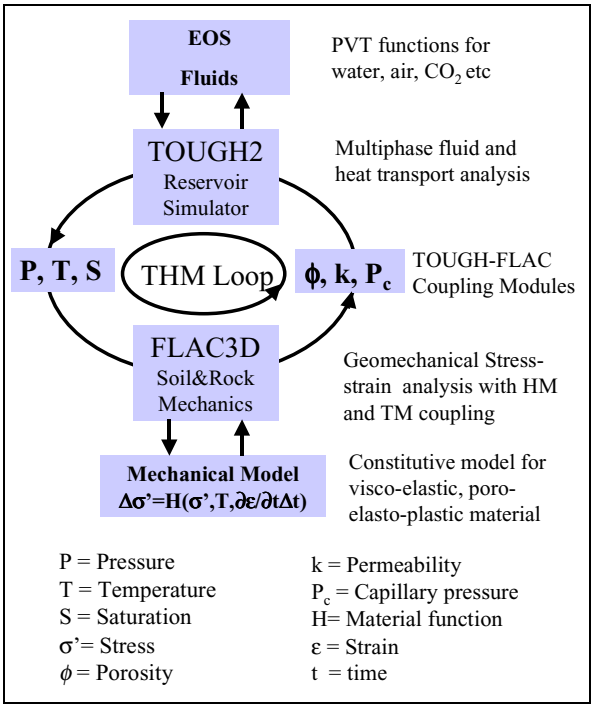

Figure 1. Schematic of linking TOUGH2 and FLAC3D for a coupled THM simulation.

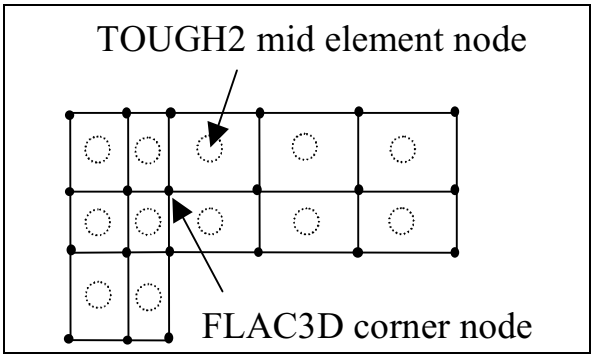

Figure 2. Coexisting TOUGH2 and FLAC3D mesh for a coupled THM simulation.

After data transfer, FLAC3D internally calculates thermal expansion and effective stress according to:

$$\Delta\boldsymbol{\varepsilon}^{T} = \mathbf{I}\beta_T \Delta T \quad (1)$$

$$\boldsymbol{\sigma}' = \boldsymbol{\sigma} + \mathbf{I}\alpha P \quad (2)$$

where $\boldsymbol{\varepsilon}^{T}$ is thermal strain β_T is the linear thermal expansion coefficient, $\mathbf{I}$ is the unit tensor, T is temperature, $\boldsymbol{\sigma}'$ is effective stress, $\boldsymbol{\sigma}$ is total stress, α is a Biot effective stress parameter (Biot, 1941) and P is pore fluid pressure. In a multiphase flow calculation, the value of P transferred to FLAC3D could represent an average pore pressure calculated from the pressures of the various phases (Rutqvist et al., 2002).

An FLAC to TOUGH link takes element stress or deformation from FLAC3D and corrects element porosity, permeability, and capillary pressure for TOUGH2 according to the following general expressions:

$$\phi = \phi(\boldsymbol{\sigma}', \boldsymbol{\varepsilon}) \quad (3)$$

$$\mathbf{k} = \mathbf{k}(\boldsymbol{\sigma}', \boldsymbol{\varepsilon}) \quad (4)$$

$$P_c = P_c(\boldsymbol{\sigma}', \boldsymbol{\varepsilon}) \quad (5)$$

No interpolation in space is required for this data transfer because stress and strain are defined in FLAC3D elements, which are identical to TOUGH2 elements. A TOUGH-FLAC coupling module for this link should calculate the hydraulic property changes, based on material-specific theoretical or empirical functions.

TOUGH-FLAC NUMERICAL PROCEDURE

A separate batch program can control the coupling and execution of TOUGH2 and FLAC3D for the linked TOUGH-FLAC simulator. In this case, it was done within the FLAC3D input file using the FLAC-FISH programming language (Itasca Consulting Group 1997). The calculation is stepped forward in time with the transient TH analysis in TOUGH2, and at each time step or at the TOUGH2 Newton iteration level, a quasi-static mechanical analysis is conduced with FLAC3D to calculate stress-induced changes in porosity and intrinsic permeability. The resulting THM analysis may be explicit sequential, meaning that the porosity and permeability is evaluated only at the beginning of each time step, or the analysis may be implicit sequential, with permeability and porosity updated on the Newton iteration level towards the end of the time step using an iterative process.

In the explicit sequential procedure (Figure 3), the TOUGH2 code is executed for a TH analysis between time t^k to t^{k+1} until mass conservation is assured by solving the TOUGH2 flow and heat equation:

$$R_n^{(\kappa)k+1} \equiv M_n^{(\kappa)k+1} - M_n^{(\kappa)k} - \frac{\Delta t}{V_n}\left\{\sum_m A_{nm} q_{nm}^{(\kappa)k+1} + V_n Q_n^{(\kappa)k+1}\right\} \quad (6)$$

where subscripts n and m label element and element face, R is the residual, M is mass or energy per unit volume, V is element volume, A is area of element face, q is flux and Q is the source term.

During this time step, the porosity and permeability are assumed to be constant, according to the values evaluated at the beginning of a time step. The mass term, $M_n^{(\kappa)k}$ in Equation (6), represents the conditions at the end of the previous time step and should therefore include the previous porosity ϕ^k. On the other hand, the mass term $M_n^{(\kappa)k+1}$ and the flux $q_{mn}^{(\kappa)k+1}$ should include the new porosity ϕ^{k+1} and the new permeability k^{k+1}, which were evaluated at the beginning of the time step. In addition, the phase saturation, S_ψ, should be corrected for the imposed change in porosity according to:

$$S_l^k = S_l^{k+1} \frac{\phi^k}{\phi^{k+1}} \quad (7)$$

$$S_g^{k+1} = 1 - S_l^{k+1} \quad (8)$$

The explicit sequential solution should be accurate if the porosity and permeability varies slowly with time or if time step size relatively small. For example, when modeling coupled THM processes around a nuclear waste repository, it is expected that slowly evolving thermal strains cause most changes in porosity and permeability. On the other hand, when modeling problems with significant strain rate and "hydraulic squeezing", time steps must be limited for an accurate solution. When using the implicit sequential scheme there is no time limitations for accuracy, however, large time steps may induce numerical stability problems.

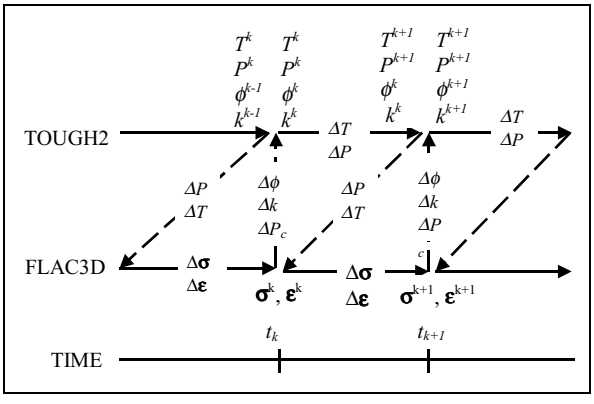

Figure 3. Numerical procedure of a linked TOUGH2 and FLAC3D simulation with explicit sequential solutions

APPLICATION OF TOUGH-FLAC

Two recent application examples demonstrate the capability of a linked TOUGH-FLAC simulation. The first example is related to sequestration of CO_2 green-house gas in brine aquifers (Rutqvist and Tsang, 2002), and the second is related to a high temperature nuclear waste repository in unsaturated rock. Within each application, material specific hydromechanical coupling relationships are developed and applied.

CO_2 sequestration into a brine formation

In this example, the TOUGH-FLAC code is applied to simulate an injection operation for disposal of CO_2 into a permeable brine formation, which is overlain by a semi-permeable caprock. The problem domain is a two-dimensional cross-section according to Figure 4a and the material properties are listed in Table 1. The injection takes place at a depth of 1,500 meters so that the CO_2 is within the temperature and pressure range for it to be a supercritical fluid. As a supercritical fluid, the CO_2 behaves like a gas with low viscosity but having a liquid-like density of 200–900 kg/m^3, depending on pressure and temperature. Because the supercritical CO_2 is less dense than water, deep underground disposal requires that the caprock is sufficiently impermeable to trap the injected CO_2 for a sufficiently long time. Important rock-mechanical aspects of this simulation are to study the integrity of the caprock and the possibilities of rock failure.

In this application the isotropic hydraulic properties are corrected using empirical porosity-mean stress and a permeability-porosity relationship (Rutqvist and Tsang, 2002). The porosity, ϕ, is related to the mean effective stress, σ'_M as

$$\phi = \phi_r + (\phi_0 - \phi_r)\exp(a \cdot \sigma'_M) \qquad (9)$$

where ϕ_0 is porosity at zero stress, ϕ_r is residual porosity at high stress, and the exponent a should be experimentally determined.

The permeability is correlated to the porosity according to the following exponential function (Rutqvist and Tsang, 2002):

$$k = k_0 \exp[c(\phi/\phi_0 - 1)] \qquad (10)$$

where k_0 is permeability at zero stress and the exponent c should be experimentally determined.

In addition to the two coupling relationships in Equations (9) and (10), the capillary pressure is modified with permeability and porosity according to a function by Leverett (1941):

$$P_c = P_{c0}(S_l)\frac{\sqrt{k_0/\phi_0}}{\sqrt{k/\phi}} \qquad (11)$$

The parameters for the porosity-mean stress and permeability-porosity relationship—ϕ_0, ϕ_r, b, c in Equations (9) and (10)—were determined to represent laboratory data by Davis and Davis (1999), which shows a one-order-of-magnitude reduction in permeability from zero to 30 MPa effective stress.

Figure 4b presents the calculated injection pressure during a 15-year injection period, with or without consideration of the stress-dependent rock mass permeability. The difference in injection pressure is explained by permeability in the injection zone (in the former case) increasing because of a general reduction in effective stresses. However, the changes in permeability are moderate (less than a factor 2) because of a rather insensitive stress-permeability relationship for the porous sandstone.

Calculated results after 10 years of injection are presented in Figures 5 to 8. These results are selected to show how a TOUGH-FLAC simulation can be used to evaluate the caprock integrity at a CO_2 injection site.

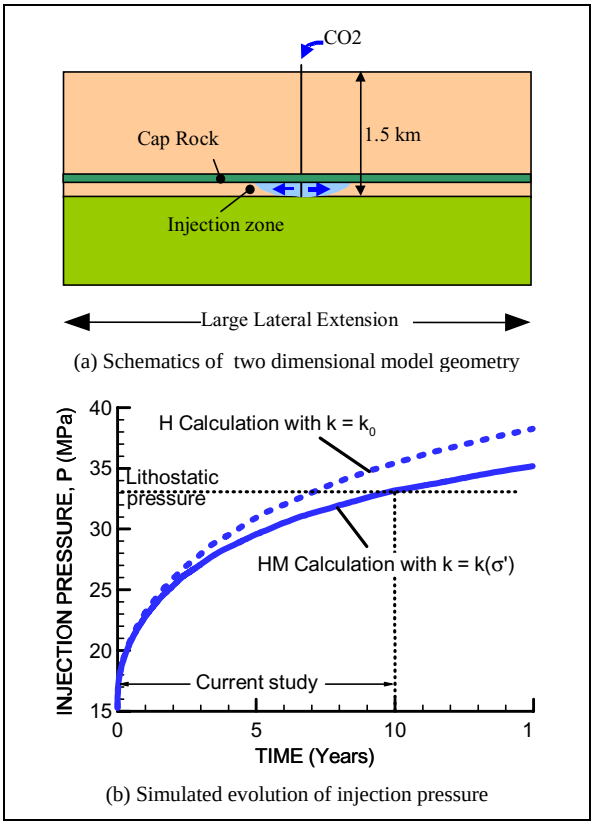

Figure 4. TOUGH-FLAC simulation of CO_2 injection into a brine water formation.

Table 1. Rock properties for simulation of CO_2 disposal in a brine formation

Property	Cap	Aquifer
Young's modulus, E (GPa)	5	5
Poisson's ratio, ν (-)	0.25	0.25
Saturated rock density, ρ_s (kg/m^3)	2260	2260
Zero stress porosity, ϕ_0 (-)	0.01	0.1
Residual porosity, ϕ_r (-)	0.009	0.09
Zero stress permeability, k_0 (m^2)	1×10^{-17}	1×10^{-13}
Irreducible gas saturation Corey's (1954) relative permeability function (-)	0.05	0.05
Irreducible liquid saturation for Corey's (1954) relative permeability function (-)	0.3	0.3
Air-entry pressure for van Genuchten's (1980) retention curve (kPa)	3100	19.6
Exponent, m for van Genuchtens's (1980) retention curve	0.457	0.457
Exponent for Equation (9), a (1/Pa)	5×10^{-8}	5×10^{-8}
Exponent for Equation (10), c	22.2	22.2
Biot's parameter in Equation (2), α	1.0	1.0

The integrity of the caprock could be jeopardized by a mechanical failure, which could occur as a result of hydraulic fracturing or reactivation of pre-existing shear fractures. These failure mechanisms are driven by changes in effective stresses, which in turn depends on the in situ stresses and injection fluid pressure.

Figure 5 presents the spread of the CO2 fluid and the fluid pressure within the aquifer/caprock system after 10 years of injection. The figure shows that the CO_2 has spread under the cap over 4 km and has penetrated upwards into the caprock by about 10 meters. At this time the injection pressure has increased to a 33 MPa, which is slightly less than the lithostatic stress at the injection point (Figure 4b).

Figure 6 shows how the vertical and horizontal in situ stresses (total stresses) increases near the injection point. The in situ stresses increases as a result of poro-elastic stresses that occurs when the porous rock attempts to expand in a confined rock mass. Both vertical and horizontal stresses increases in the injection aquifer. However, in the cap-rock, just above the injection interval, the horizontal stresses increases much more than the vertical stresses.

Figure 7 presents the changes in vertical and horizontal effective stress near the CO2 plume. The figure shows that the effective stresses are reduced mostly at the interface between the injection aquifer and the caprock and the vertical effective stress is reduced more than the horizontal one.

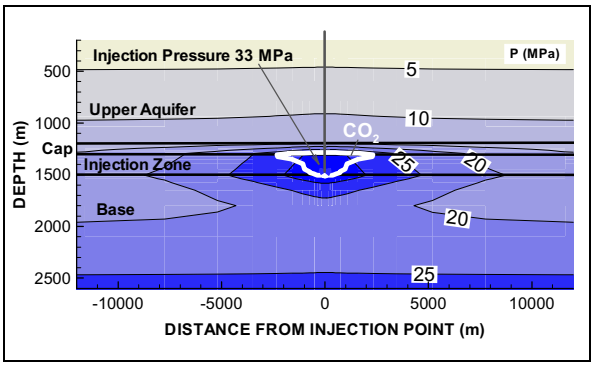

Figure 5. Calculated fluid pressure distribution and the spread of the CO2 plume after 10 years of injection.

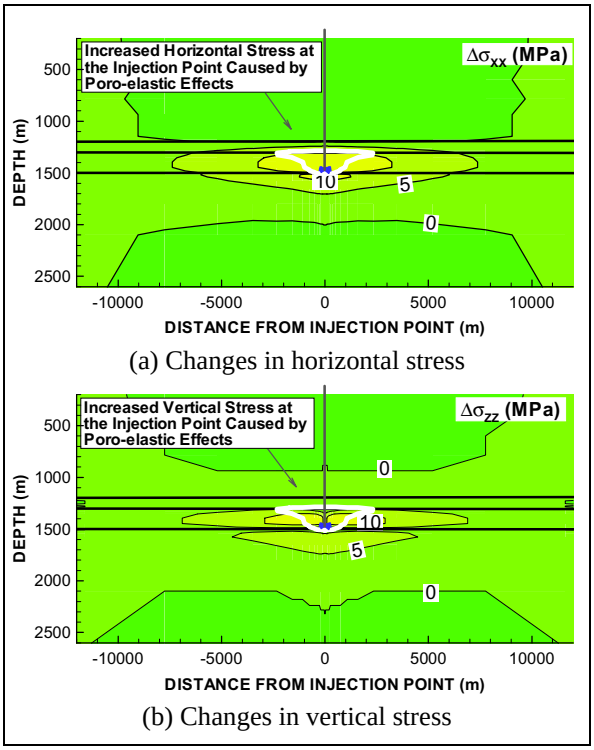

Figure 6. Calculated changes in total in situ stresses after 10 years of injection.

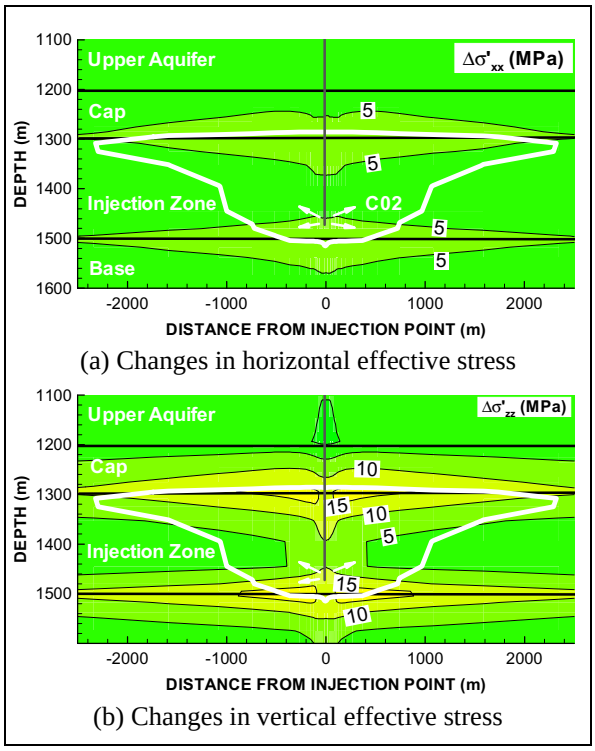

(a) Changes in horizontal effective stress

(b) Changes in vertical effective stress

Figure 7. Calculated Changes in effective stress in the aquifer-cap rock system after 10 years of CO_2 injection.

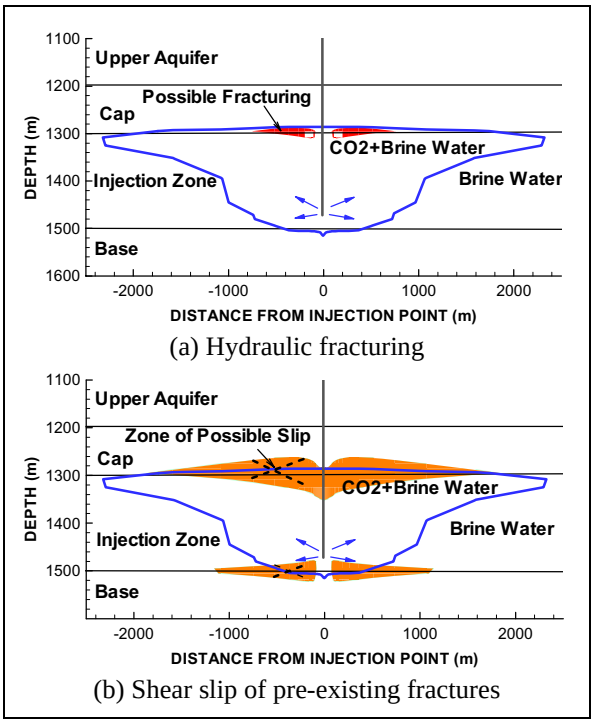

(a) Hydraulic fracturing

(b) Shear slip of pre-existing fractures

Figure 8. Zones where the mechanical failure could occur calculated at 10 years of injection.

Figure 8 shows that if mechanical failure occurs it would most likely initiates at the interface between the caprock and injection the zone. In this zone, the reduction in vertical effective stress can lead to the formation of horizontal hydraulic fractures (Figure 8a). Furthermore, a larger zones of possible slip on pre-existing fractures occurs at the upper and lower part of the injection zone. This implies that an unfavorably oriented fault could be reactivated with accompanying micro-seismicity and possible permeability change. However, even if fracturing or fault reactivation would take place in the lower parts of the caprock, the TOUGH-FLAC simulation indicates that it would be contained within the lower portion of the cap and would not propagate through the upper part of the cap.

This application example demonstrates how the specially developed capabilities of the TOUGH2 code for the complex behavior of the supercritical CO_2 could be utilized in a coupled TOUGH-FLAC simulation. These results contribute to identifying the most critical mechanisms for the integrity and long-term stability of a CO_2 injection site. Further studies include effects of a permeable fault (Rutqvist and Tsang, 2002), heterogeneous reservoir rock, and inelastic aquifer compaction behavior.

Coupled THM analysis of a high temperature heater test in semi-dry fractured rocks

In this example, TOUGH-FLAC is applied for a coupled THM simulation of the Yucca Mountain Drift Scale Test (DST). The DST is a large-scale, long-term high-temperature thermal test designed to investigate coupled thermal-mechanical-hydrological-chemical behavior in an unsaturated, fractured, and welded tuff rock mass. The DST centers around a heated drift, which is 5 meters in diameter and has a 47.5 m long heated section. Heating is provided by nine drift heaters within the heated drift, as well as 50 rod heaters, referred to as “wing heaters,” placed into horizontal boreholes emanating from the heated drift (Figure 9a). The DST is simulated with TOUGH-FLAC in a two dimensional cross section oriented normal to the drift axis (Figure 9a). The highly fractured rock mass at the test site is modeled as a dual-permeability medium, which consists of interacting matrix and fracture continua.

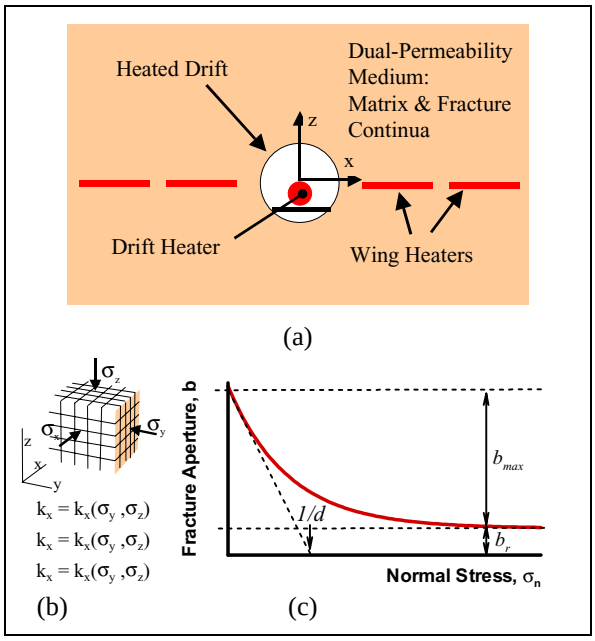

Figure 9. TOUGH-FLAC simulation of the Yucca Mountain Drift Scale Test (a) Schematics of two-dimensional model geometry. (b) Conceptual model for stress-permeability coupling. (c) Normal stress-aperture relationship for fractures.

For the Yucca Mountain site, the correction of hydraulic properties with stress are based on a conceptual model of a highly fractured rock mass that contains three orthogonal fracture sets as shown in Figure 9b (Rutqvist and Tsang, 2003). The porosity and permeability-correction factors are calculated from the initial and current apertures in Fracture Set 1, 2, and 3 according to:

$$F_{\phi} = \frac{b_1 + b_2 + b_3}{b_{1i} + b_{2i} + b_{3i}} \tag{12}$$

$$F_{kx} = \frac{b_2^3 + b_3^3}{b_{2i}^3 + b_{3i}^3}, F_{ky} = \frac{b_1^3 + b_3^3}{b_{1i}^3 + b_{3i}^3}, F_{kz} = \frac{b_1^3 + b_2^3}{b_{1i}^3 + b_{2i}^3} \tag{13}$$

where fractures in Fracture Sets 1, 2, and 3 are assumed to be equally spaced and oriented normal to x, y, and z directions, respectively, and a parallel-plate fracture flow model (Witherspoon et al. 1980) is adopted. The capillary pressure is corrected with porosity and permeability changes according to the Leverett (1941) function:

$$F_{Pc} = \sqrt{\frac{F_k}{F_{\phi}}} \tag{14}$$

where

$$F_k = \sqrt[3]{F_{kx} \times F_{ky} \times F_{kz}} \tag{15}$$

In this study, the current fracture aperture b depends on the current effective normal stress σ'_n, according to the following exponential function (Rutqvist and Tsang, 2003):

$$b = b_r + b_m = b_r + b_{\max}\left[\exp\left(d\sigma'_n\right)\right] \tag{16}$$

where b_r is a residual aperture, b_m is mechanical aperture, b_{max} is the maximum mechanical aperture, and d is a parameter related to the curvature of the function (Figure 9c). This expression can be inserted into Equation (13) to derive expressions for rock mass permeability-correction factors in x, y and z directions

Calculated results after 12 months of heating are presented in Figures 10 to 13. These results are selected to illustrate how TOUGH-FLAC can be utilized to calculate THM-induced changes in air-permeability in fractured rocks. Changes in air-permeability are particular important because they are largely dependent on stress-induced changes in fracture permeability, which is a key process in coupled THM modeling of fractured rocks.

Figure 10 shows that after 12 months of heating the temperature has reached above the boiling temperature around the heated drift and near the wing heaters. The high temperature induces strong thermal-hydrological processes with evaporation of liquid water near the heatsource (Figure 11). The evaporated water is transported as vapor away from the heat source toward cooler regions where it is condensed to liquid water (Figure 11). As a result, a dry-out zone is created near the heat source and a condensation zone is progressively moving away from the heat source. In the condensation zone, an increase in fractures moisture content should result in a decrease air-permeability.

The high temperatures shown in Figure 10 gives rise to thermal expansion of the rock mass with associated thermal stresses (Figure 12). Near the heat source, the horizontal compressive stresses increases strongly with a maximum at the drift wall and near the heat sources. Such increase in compressive stresses tends to tighten fractures to smaller aperture leading to a reduction in air-permeability. Away from the heat source, the horizontal stresses decreases slightly (Figure 12). A reduction in horizontal stresses will tend to open pre-existing vertical fractures to a larger aperture leading to an increase in air-permeability.

Table 2. Rock properties for simulation of a heater test in fractured welded tuff.

	Property	Value
Matrix Hydraulic and Thermal Properties	Permeability	1.24E-17 m^2
	Porosity	0.11
	van Genuchten, α_m	2.25E-6 Pa^{-1}
	van Genuchten m_m (or λ)	0.247
	Residual saturation	0.18
	Rock grain density, ρ	2530 kg/m3
	Rock grain specific heat	953 J/kg K)
	Dry thermal conductivity	1.67 W/m K
	Wet thermal conductivity	2.0 W/m K
Fracture Hydraulic and Hydro-mechanical Properties	Permeability, k	1.00E-13 m^2
	Porosity	0.263E-3
	van Genuchten, α_f (1/Pa)	9.73E-5 Pa^{-1}
	van Genuchten, m_f (-) (or λ)	0.492
	Residual saturation	0.01
	Fracture frequency	4.32 m^{-1}
	Initial fracture aperture, b_f	51.8 µm
	b_{max} for Equation (16)	150 µm
	Exponent *d* for Equation (16)	0.6 MPa^{-1}
Rock Mass Mechanical Properties	Young's Modulus	14.77 GPa
	Poission's ratio	0.21
	Thermal Expansion Coefficient, β_T	5+0.0583×T 10^{-6}/°C

Figure 13 presents the calculated THM-induced changes in air-permeability. These changes in air-permeability are caused by the combined effect of thermally induced changes in fracture moisture content (Figure 11) and stress-induced fracture aperture changes (Figure 12). Near the heat source, the permeability decreases mainly because of fracture closure, but is also affected by thermally induced wetting and drying. Away from the heat source, a zone of increased permeability has developed as results of opening of vertical fractures.

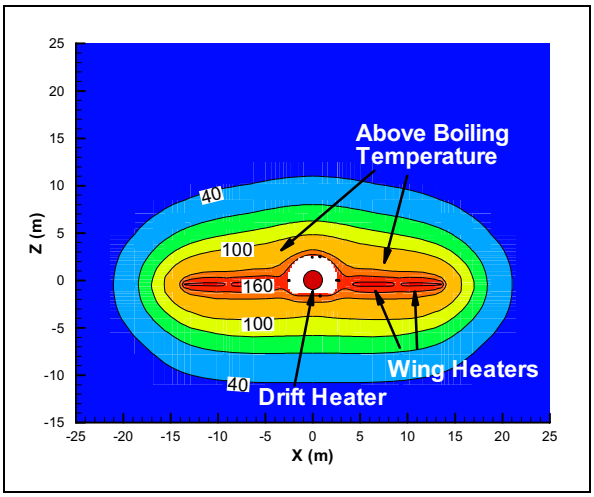

Figure 10. Calculated temperature distribution after 12 months of heating.

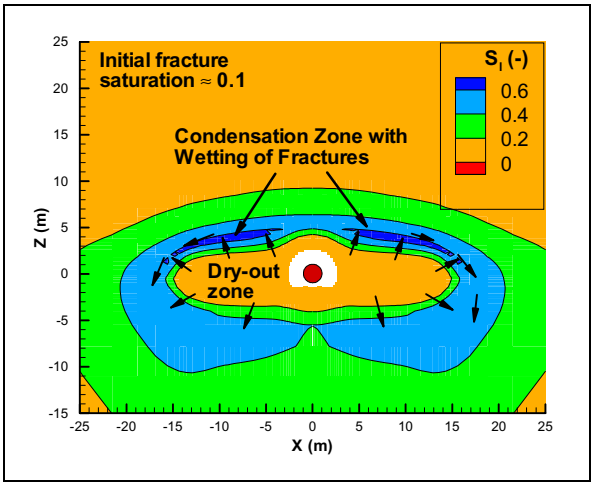

Figure 11. Calculated liquid saturation in fractures after 12 months of heating.

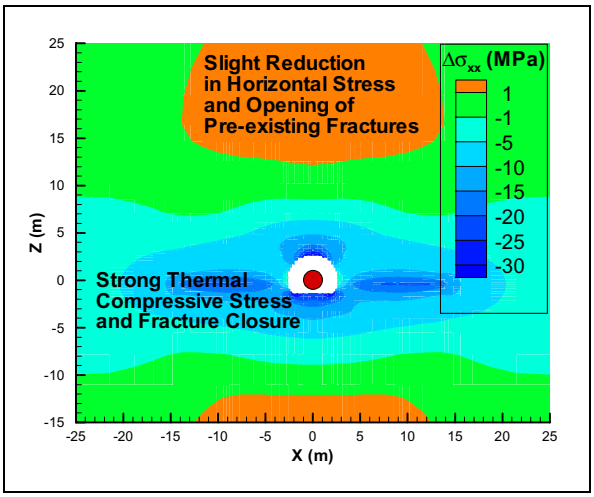

Figure 12. Calculated thermally induced horizontal stresses after 12 months of heating.

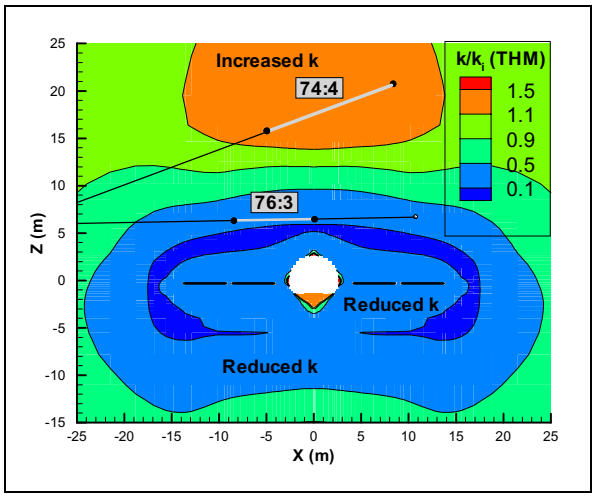

Figure 13. Calculated changes in air-permeability as a result of TH induced changes liquid fracture saturation and TM induced changes in fracture aperture. 74:4 and 76:3 are borehole sections at which calculated and measured air-permeability is compared in Figure 14.

Figure 14 presents a comparison of calculated and measured air-permeability at two borehole sections. The calculated changes in air-permeability is in good agreement with the measured ones both in trends and magnitude. The good agreement between the calculated and measured results shows that the adopted conceptual model for stress induced changes in permeability depicted in Figure 9 is sound and validates the numerical values of b_{max} and *d* that defines the normal stress-aperture function in Figure 9c.

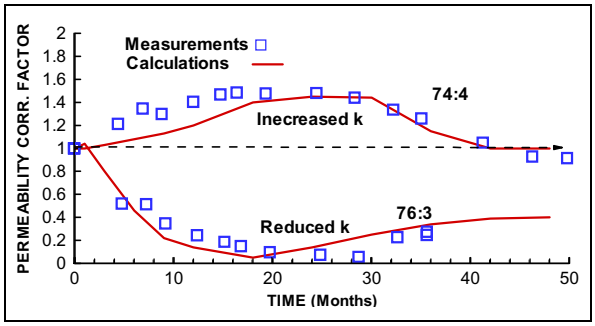

Figure 14. Calculated and measured permeability correction factor F_k (see Equation 15 for definition of F_k).

In this example, we could utilize the capabilities of the TOUGH2 code to simulate complex above boiling two-phase flow behavior—for efficiency, this requires special treatment with exchange of primary variables in the numerical solution (Pruess et al., 1999)—and a full THM simulation was achieved through coupling with the FLAC3D code. More long-term results and the impact of these processes on the performance of a potential repository at Yucca Mountain are discussed in Rutqvist and Tsang (2003).

CONCLUDING REMARKS

We have linked two codes—TOUGH2 and FLAC3D—for analysis of coupled THM processes in complex geological media. The codes were linked with modules representing the coupled thermo-mechanical and hydrologic-mechanical behavior of rocks. The coupling modules contain nonlinear stress versus permeability functions, which were calibrated against site-specific data. These coupling modules could be exchanged with modules containing any other type of empirical or theoretical hydrologic-mechanical coupling relationship. We have demonstrated the usefulness of linked, sequentially coupled THM analyses for complex problems related to injection and storage of CO_2 in brine aquifer formations and to the expected conditions at a high temperature nuclear waste disposal in unsaturated rock. In both these examples, the hydromechanical changes are relatively slow, which is most suitable for the sequentially explicit solution. Problems with higher strain rates relative to fluid mobility may require the sequential implicit approach or ultimately a fully implicit coupled approach.

ACKNOWLEDGMENT

Technical review and comments by Dr. Kazumasa Ito and Dr. Guomin Li, Lawrence Berkeley National Laboratory are much appreciated. This work was jointly supported by the Director, Office of Science, Office of Basic Energy Sciences, Division of Chemical Sciences, Geosciences and Biological Sciences, of the U.S. Department of Energy, under contract No. DE-AC03-76-SF00098, and by the Director, Office of Civilian Radioactive Waste Management, U.S. Department of Energy, through Memorandum Purchase Order EA9013MC5X between Bechtel SAIC Company, LLC and the Ernest Orlando Lawrence Berkeley National Laboratory (Berkeley Lab) through the U.S. Department of Energy Contract No. DE-AC03-76SF00098, and by the Swedish Nuclear Power Inspectorate.

REFERENCES

Biot, M. A., General theory of three dimensional consolidation. *J Applied Physics*, 12, 155–164, 1941.

Corey AT. The interrelation between oil and gas relative permeabilities. Producers Monthly November, 38-41, 1954.

Davis, J.P., and D.K. Davis, Stress-dependent permeability: characterization and modeling. Society of Petroleum Engineers, SPE Paper no 56813, 1999.

Itasca Consulting Group Inc. FLAC-3D Manual: Fast Lagrangian Analysis of Continua in 3 Dimensions–Version 2.0. Itasca Consulting Group Inc., Minnesota, USA, 1997.

Leverett, M.C., Capillary behavior in porous media. *Trans, AIME*, 142, 341-358, 1941.

Pruess, K., C. Oldenburg, and G. Moridis, *TOUGH2 User's Guide, Version 2.0*, Report LBNL-43134, Lawrence Berkeley National Laboratory, Berkeley, Calif., 1999.

Rutqvist, J, Y-S. Wu, C-F Tsang and G. Bodvarsson, A modeling approach for analysis of coupled multiphase fluid flow, heat transfer, and deformation in fractured porous rock, *Int. J. Rock Mech. Min. Sci.* 39, 429-442, 2002.

Rutqvist, J., and C.-F. Tsang, A study of caprock hydromechanical changes associated with CO2 injection into a brine aquifer. *Environmental Geology*, 42, 296-305, 2002.

Rutqvist, J., and C.-F. Tsang, Analysis of thermal-hydrologic-mechanical behavior near an emplacement drift at Yucca Mountain. *J. Contaminant Hydrology* (In press), 2003.

van Genuchten MT. A closed-form equation for predicting the hydraulic conductivity of unsaturated soils. *Soil Sci Soc Am J* 1980;44:892-898.

Witherspoon, P.A., J.S.Y. Wang, K. Iwai and J.E. Gale. Validity of the cubic law for fluid flow in a deformable fracture. *Water Resour. Res*. 1980;16:1016-1024.